„Meteor" Forsch.-Ergebnisse	Reihe A	No. 16	Seite 23–34	Berlin · Stuttgart	Juli 1975

On the Mediterranean outflow west of Gibraltar*

by

Walter Zenk, Institut für Meereskunde, Kiel

With 9 figures and 1 table

Zur Ausbreitung des Mittelmeerwassers westlich von Gibraltar

Zusammenfassung

Ausführliche Untersuchungen zum Problem der Wasserverteilung und -vermischung des mediterranen Ausstromes im Golf von Cádiz wurden im Frühjahr 1971 während der „Meteor"-Fahrt 23 durchgeführt. Die Beobachtungsergebnisse stützen sich hauptsächlich auf Hydrosondenstationen, auf Strom- und Temperaturmessungen von verankerten Geräten und auf geologische Untersuchungen von Kenyon & Belderson (1973). Der Leitcharakter der Bodenmorphologie, der zur Aufspaltung des Ausstromes führt (Madelain 1970), wurde prinzipiell bestätigt. Wenigstens vier Kanäle konnten durch Beobachtungen belegt werden. Für drei von diesen wird ein Schätzwert für die mittlere Ausstrommenge angegeben. Danach werden durch den nördlichen schelfnahen Ausstromkanal $0{,}40 \cdot 10^6$ m^3 sec^{-1} transportiert. Der Hauptausstrom verläßt den Golf von Cádiz in südwestlicher Richtung. Die Transportmenge beträgt hier $1{,}39 \cdot 10^6$ m^3 sec^{-1}. Eine weitere Menge in Höhe von $0{,}24 \cdot 10^6$ m^3 sec^{-1} erreicht den tiefen Atlantik durch ein Tal zwischen den zuvor genannten Ausstromkanälen. In einem stationären Vermischungsmodell wird gezeigt, daß $0{,}95 \cdot 10^6$ m^3 sec^{-1} reines Mittelmeerwasser verdünnt mit $1{,}97 \cdot 10^6$ m^3 sec^{-1} Atlantikwasser den Golf von Cádiz verlassen.

Summary

During "Meteor" cruise 23 in spring 1971 intensive investigations of the Mediterranean outflow in the Gulf of Cádiz were carried out. In order to give a budget of the inflow and outflow numerous CTD-stations were taken. The observations also included six moored current meter arrays deployed in the known outflow channels. The considerations given here are based mainly on three hydrographic sections, current meter records averaged over one month, and geological observations from the bed forms beneath the Mediterranean undercurrent. The results show that the outflow essentially is determined by the bathymetry of the area. At least four separate outflow channels could be confirmed. The volumentric transport rates of three of them were calculated. These channels are the northerly near shelf branch ($0.40 \cdot 10^6$ m^3 sec^{-1}), the main branch ($1.39 \cdot 10^6$ m^3 sec^{-1}) in southwesterly direction, and an intermediate branch ($0.24 \cdot 10^6$ m^3 sec^{-1}) found between both. In a static box model the progressive mixing of $0.95 \cdot 10^6$ m^3 sec^{-1} pure Mediterranean Water with $1.97 \cdot 10^6$ m^3 sec^{-1} North Atlantic Central Water is demonstrated.

Introduction

The constant exchange of Atlantic and Mediterranean Water masses in the Strait of Gibraltar has been a subject of scientific research since at least 1661 when the Royal Society of London approved an expedition for the investigation of the current system in the Strait (see Deacon 1971).

During the 19th century it became well accepted that the steady inflow of Atlantic Water through the Strait of Gibraltar is balanced by evaporation in the Mediterranean Sea and by an outflow beneath the surface inflow. The warm and highly saline undercurrent sinks due to its high density until it reaches a level of equilibrium in the Atlantic water.

* Contribution number 3497 from the Woods Hole Oceanographic Institution

At this point it begins to spread horizontally and forms the upper deep water of the Atlantic Ocean with its typical intermediate maxima in temperature and salinity.

An overall view of the hydrography east and west of the Strait of Gibraltar was shown by SCHOTT (1915, 1928) and has been recently repeated with new data by STOMMEL et al. (1973). Both longitudinal sections through the Strait depict the warm and highly saline outflow west of the sill as a relatively thin bottom layer which begins to spread horizontally at approximately 1000 m depth.

The present paper deals with the distribution of the Mediterranean outflow in the Gulf of Cádiz. The work is based mainly on observational results that were obtained during the Northeast Atlantic Expedition of R/V "Meteor" in the spring of 1971. The complete logistics of the cruise have been reported by SIEDLER (1972) including station and mooring positions and durations of the records. The CTD instrument used is of the Multisonde type and has been described by KROEBEL (1973). A complete set of the current meter logs with time series and amplitude spectra has been released in a separate paper (ZENK 1974).

The same subject was investigated by HEEZEN & JOHNSON (1969) with special emphasis on the interaction between the undercurrent and the bottom microphysiography. Our knowledge of this interaction recently was improved by KENYON & BELDERSON (1973) who showed by means of side-scan sonar technique the tracing of the undercurrent on the sea floor. From these and various additional sources (GIESEL & SEIBOLD 1968; SWALLOW 1969; ZENK 1971; THORPE 1972, 1973; FUGLISTER, unpublished IGY-data) a rather complete picture of the distribution of the undercurrent in the Gulf of Cádiz can be obtained (Fig. 1). After leaving its source the outflow turns northwestward at about 35° 50′ W 06° 40′ N and is focused in a narrow stream. Further north the outflow splits into several channels. One of these follows the outer edge of the Iberian continental shelf while the rest flows into several southwesterly and northwesterly canyons.

Less, however, is known about the quantitative distribution of the total outflow in these various channels. The following observations can supply a more detailed understanding of the situation leading to the outflow cascade with some quantitative values.

The distribution of the undercurrent in the Gulf of Cádiz

The influence of the bathymetry of the Gulf of Cádiz on the Mediterranean undercurrent is at least as important for the formation of the Upper Deep Atlantic Water as the topography of the Strait of Gibraltar itself. The reason for this is the combined effect of the following factors. The undercurrent is marked by high velocity which is strongly orientated by direct contact with the sea floor. The topography of the Gulf of Cádiz can be described as a system of ridges, canyons, and broad terraces in the continental slope. As a consequence of the high current speed the undercurrent is strongly influenced by Coriolisforce and entrainment processes. The sloping topography accelerates the outflow with its higher density relative to the surrounding North Atlantic Central Water.

Intensive theoretical studies on steady overflows with the Mediterranean as an example were published by SMITH (1973). In this work the observations of MADELAIN (1970) on the topographic influence on the outflow were used for an intercomparison between model computations, laboratory experiments and the physical example of the Mediterranean outflow. The computations show the combined influence of entrainment and ambient stratification limiting the descent of the outflow to a depth of approximately 1200 m.

The entrance to the Gulf of Cádiz (Section A)

In order to study the outflow at its entrance into the Gulf of Cádiz a hydrographic cross section (A) was carried out at a region where the undercurrent could be expected to be undivided (Fig. 2). The observations obtained included, beside the stations of Section A, a mooring array (equipped with two thermistor chains and four current meters) and repeated CTD casts during 25 hours. An overall summary of the current meter data of all moorings discussed here is given in Table 1.

Taking the 36.0‰ isohaline and its straight extension between station 94 and the continental margin as the boundary between the highly saline undercurrent and the much less saline North Atlantic Central Water, the outflow occupies an estimated cross area of $5 \cdot 10^6$ m^2. As one can see from Fig. 2, this area is marked by strong vertical gradients in salinity and one might expect that the outflow causes a large shear zone at the boundaries. Unfortunately two of four current meters that covered the profile within current meter array 19 failed. However, with the remaining information of the mean speed from meters 19 105 and 19 102 together with thermistor chain record 19 101 and the assumption of a motionless layer at the 500-m-level in the area of the mooring, one can estimate an integrated mean speed value of 35 cm sec^{-1}. This estimate corresponds to an average flux through

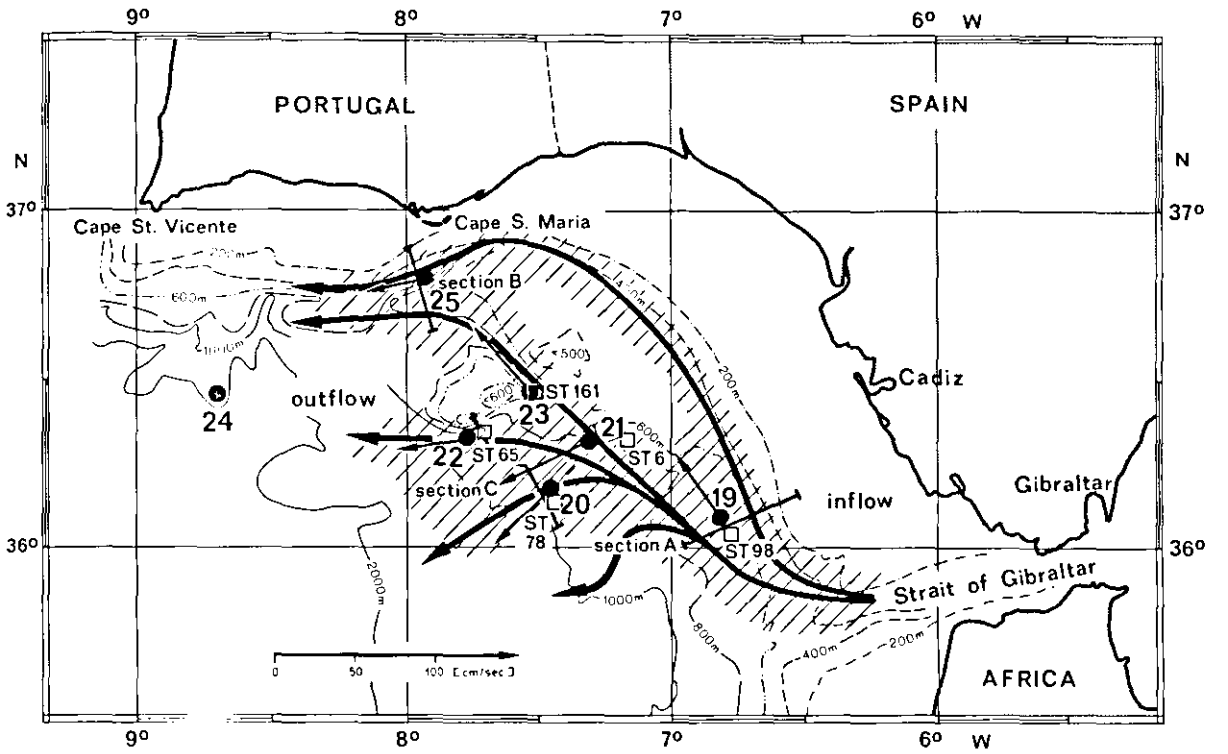

Fig. 1. Distribution of the Mediterranean undercurrent in the Gulf of Cádiz. Dots and squares show the position of mooring sites and CTD stations, respectively.

Abb. 1. Verteilung des Mediterranen Unterstromes im Golf von Cádiz. Punkte kennzeichnen die Lage der Strommesser-Verankerungen, Quadrate die der CTD-Stationen.

Table 1 Mean current and temperature data from the Golf of Cádiz as obtained during "Meteor" cruise 23. For detailed data information, see ZENK (1974).

Tabelle 1 Mittlere Strömungen und Temperaturen aus dem Golf von Cádiz nach Messungen während der „Meteor"-Fahrt Nr. 23. Ausführliche Informationen enthält eine Datenzusammenstellung von ZENK (1974).

Ref. No.	Location φ (N)	Location λ (W)	Date 1971	Depth m	Clearance Bottom m	Speed cm/sec	St. Dev. Speed cm/sec	Direction °T	Temp. °C	St. Dev. Temp. °C
19102	36° 05.4′	06° 48.9′	27. 4.–19. 5.	552	112	13	10	351	12.2	0.19
5			–27. 5.	649	15	68	7	324	13.1	0.15
21101	36° 18.1′	07° 18.1′	27. 4.–27. 5.	557	313	5	7	—	11.6	0.48
2				649	221	23	12	281	12.6	0.33
3				752	118	29	11	266	13.0	0.15
4				855	15	50	8	243	13.1	0.08
25101	36° 48.7′	07° 55.6′	29. 4.–26. 5.	456	218	40	7	252	13.5	0.49
2				547	127	39	12	259	13.8	0.15
4				616	58	25	10	259	13.6	0.13
5				659	15	20	9	264	13.5	0.17
20101	36° 10.5′	07° 27.1′	28. 4.–27. 5.	697	320	10	6	231	10.7	0.35
3				796	221	12	7	231	11.2	0.35
4				901	116	30	15	229	11.6	0.27
5				1002	15	44	13	236	12.6	0.16
22101	36° 19.0′	07° 46.2′	29. 4.–26. 5.	635	465	13	7	270	12.0	0.49
3				884	216	39	11	272	13.0	0.13
4				984	116	22	12	274	12.8	0.13
5				1085	15	9	9	272	12.6	0.09
23101	36° 28.0′	07° 31.0′	28. 4.–26. 5.	448	212	2	3	—	11.9	0.24
2				539	121	5	4	325	11.6	0.40
3				592	68	22	7	334	12.5	0.36
4				645	15	36	6	319	13.2	0.19

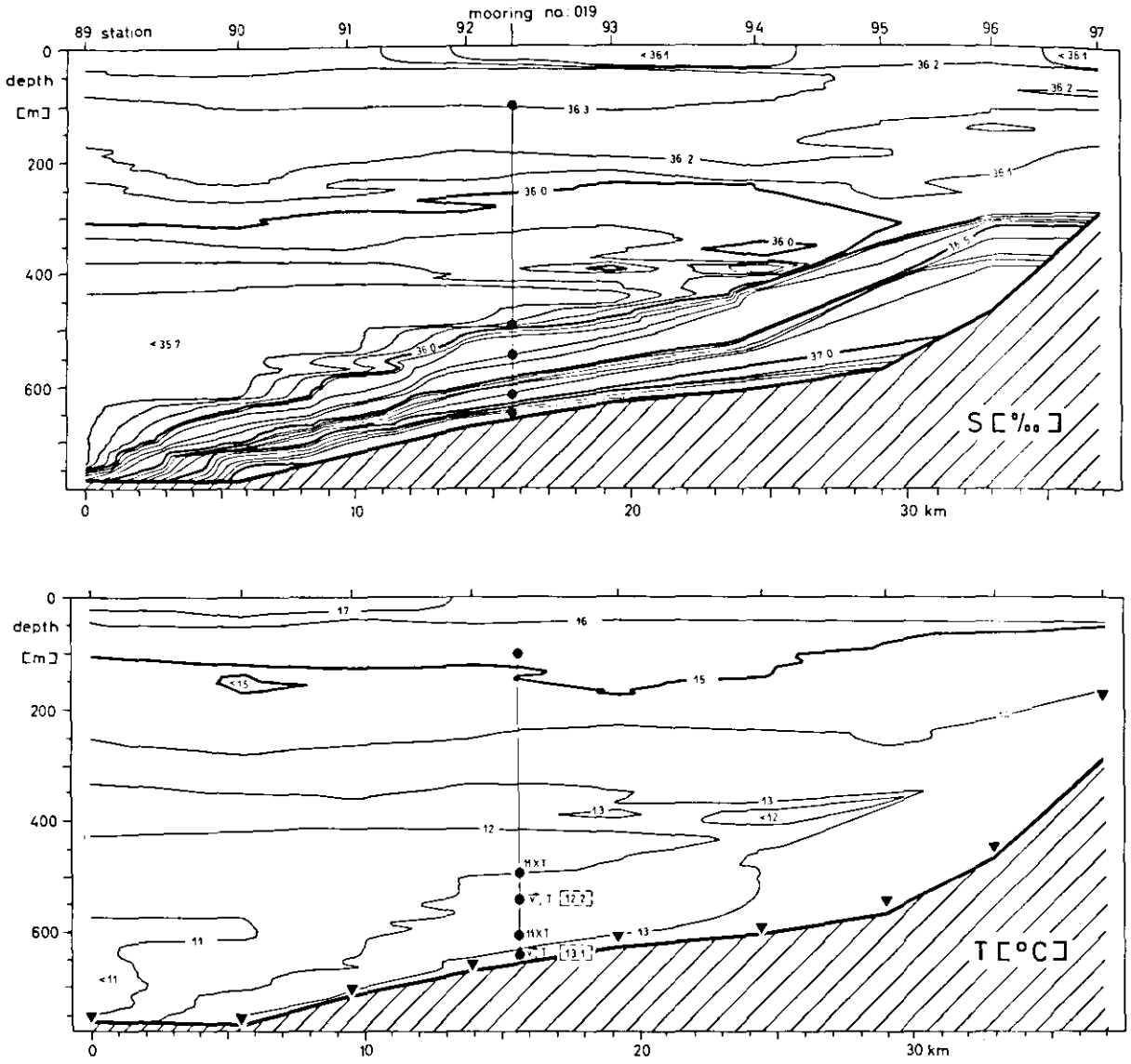

Fig. 2. Hydrographic section A through the Mediterranean outflow at its entrance into the Gulf of Cádiz. The triangles (▼) denote the lowering depth of the CTD instrument. Mooring no. 19 delivered two current meter ($\vec{V}$, T) and two thermistor chain (11 × T) records. The moored temperature values averaged over the record length (see Table 1) are shown in the dashed boxes. Linear interpolation between stations was done automatically by computer.

Abb. 2. Hydrographischer Schnitt A durch das ausströmende Mittelmeerwasser am Eingang zum Golf von Cádiz. Dreiecke (▼) kennzeichnen die maximale Einsatztiefe der Hydrosonde. Mittels Verankerung Nr. 19 konnten Registrierungen von zwei Strommessern ($\vec{V}$, T) und zwei Thermistorketten (11 × T) gewonnen werden. Die über die gesamte Registrierdauer (siehe Tabelle 1) gemittelten Temperaturwerte sind in den Kästchen angegeben. Zwischen den Stationen wurde mit Hilfe eines Rechners linear interpoliert.

Section A into the Gulf of Cádiz of approximately $T_{19} = 1.75 \cdot 10^6$ m^3 sec^{-1}.

Taking the same mixing model between pure Mediterranean Water (MW) at the sill (S_M = 38.4‰) and North Atlantic Central Water (NACW, S_A = 35.6‰) as was used in an earlier study (ZENK 1970) one finds that the undercurrent with an average salinity of S_{19} = 37.1‰ at cross section A contains roughly 54% pure MW and 46% NACW.

Typical estimates for the net outflow of pure MW in the Strait lie in the order of $T_M = 1 \cdot 10^6$ m^3 sec^{-1} (e.g. STOMMEL et al. 1973). This number corresponds to $T_{19}' = 1 \cdot 10^6$ m^3 sec^{-1}. 100/54 = $1.85 \cdot 10^6$ m^3 sec^{-1} for the location of Section A. The difference between T_{19} and T_{19}' is not surprising since the outflow in the Strait shows a wide range of variation. A measured value is not available for the time of observation at Section A.

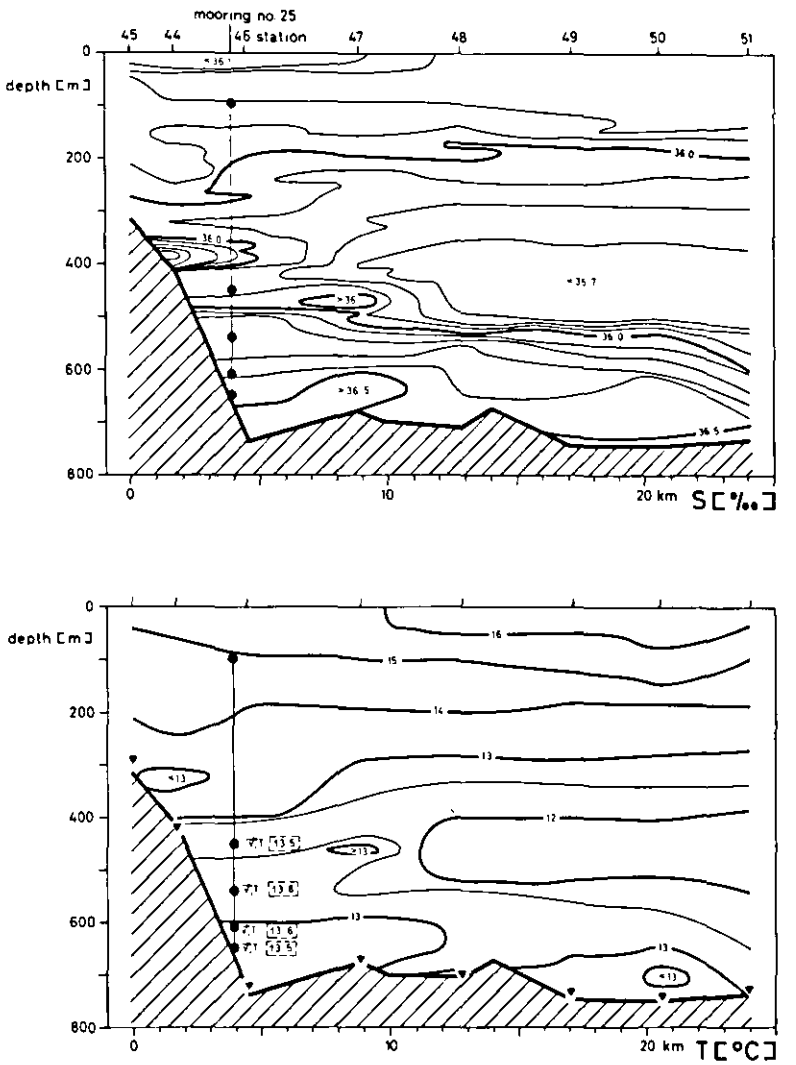

Fig. 3. Hydrographic section B south of Cape Santa Maria. The graph illustrates two separated highly saline bottom layers belonging to the shelf and to the intermediate branch of the Mediterranean outflow.

Abb. 3. Hydrographischer Schnitt B südlich von Kap Santa Maria. Zwei getrennte salzreiche Bodenschichten sind zu erkennen, die die Kerne des schelfnahen und des Zwischen-Ausstromarmes von Mittelmeerwasser bilden.

Section A is situated in an area where side-scan sonar studies of KENYON & BELDERSON have shown the transition between sand ribbons and sand waves indicating the very high speed of the undercurrent. The maximum instantaneous speed measured by mooring 19 at 15 m above the bottom was 84 cm sec^{-1} which is lower than expected. The explanation for this relatively low maximum which occurred only once during one month of recording can be given by the strong shear associated with the high salinity gradient. The data show that the instrument level was above the thin core layer. Much higher speeds immediately near the bottom were observed earlier in the sill region of the Strait (LACOMBE et al. 1968) as well as in the outflow valleys leading out of the Gulf of Cádiz (THORPE 1972). In both cases the maximum speed exceeded 100 cm sec^{-1}.

Two other features of the pattern of sedimentation are reflected in Section A. The southwestern side of the undercurrent coincides with one of the depositional ridges pointed out by KENYON & BELDERSON. The northeastern counterpart could not be found in Section A. The remarkable dilution of the core layer of the outflow between stations 95 and 96 may be explained in terms of mixing between the southward Atlantic countercurrent on the surface and the outflow. Although no direct current measurements of this continental shelf current are known, the bottom physiography showing long straight crested sand waves indicates its existence.

The shelf branch (Section B)

Soon after passing Section A the undercurrent starts to split into several branches each guided by local topographic features (MADELAIN 1970). The most northern branch which originates from the northeastern side of Section A follows the upper continental slope in a depth range of approximately 400—600 m. At about 7° 30′ W the outflow enters a channel which opens widely onto a terrace south

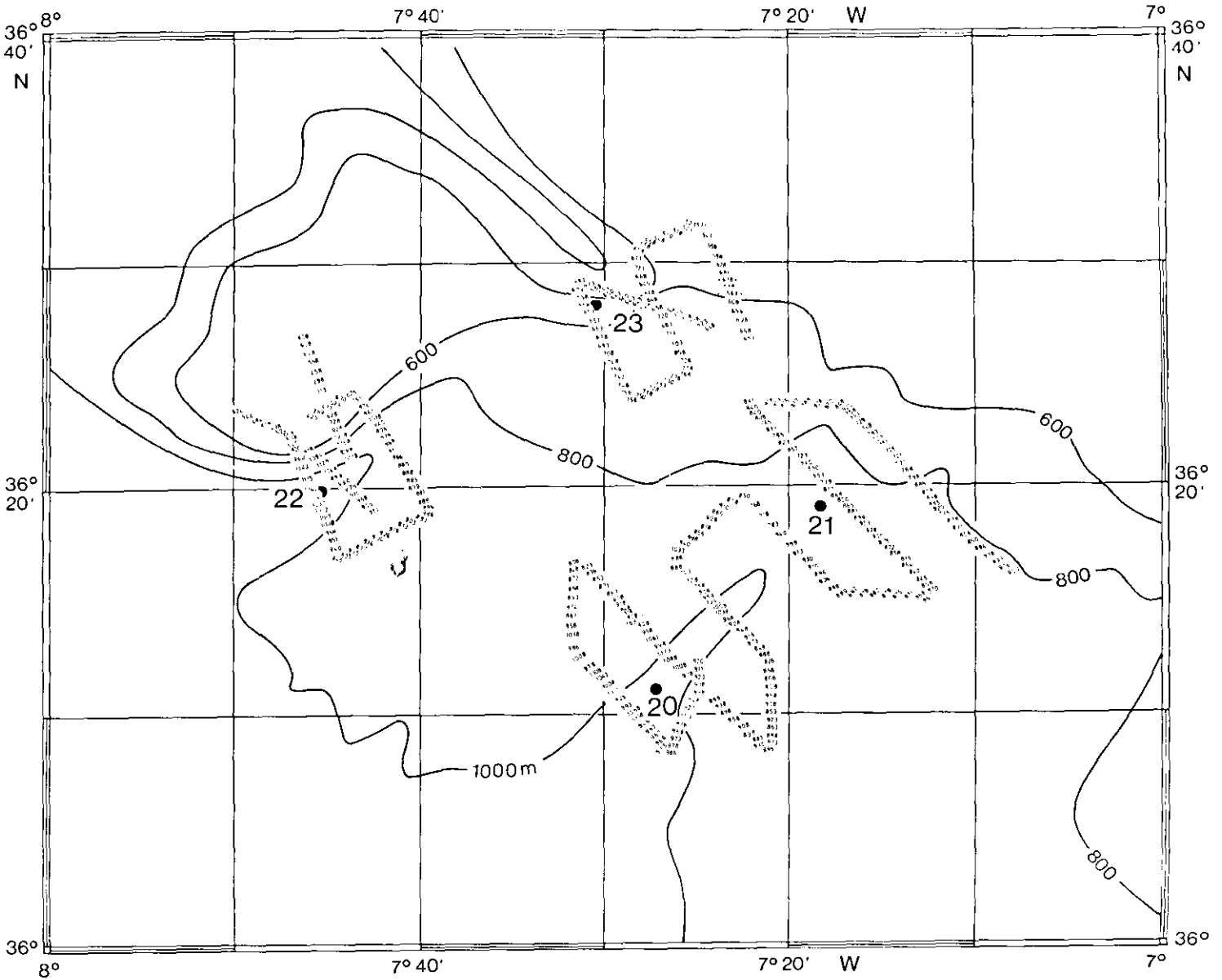

Fig. 4. Bottom topography at moorings 20—23. Here the roots of the intermediate and the main branch of the Mediterranean outflow were identified.

Abb. 4. Bodentopographie in der Umgebung von Verankerung 20—23. Hier konnten die Ausgangsgebiete des Zwischen- und des Haupt-Ausstromarmes des Mittelmeerwassers nachgewiesen werden.

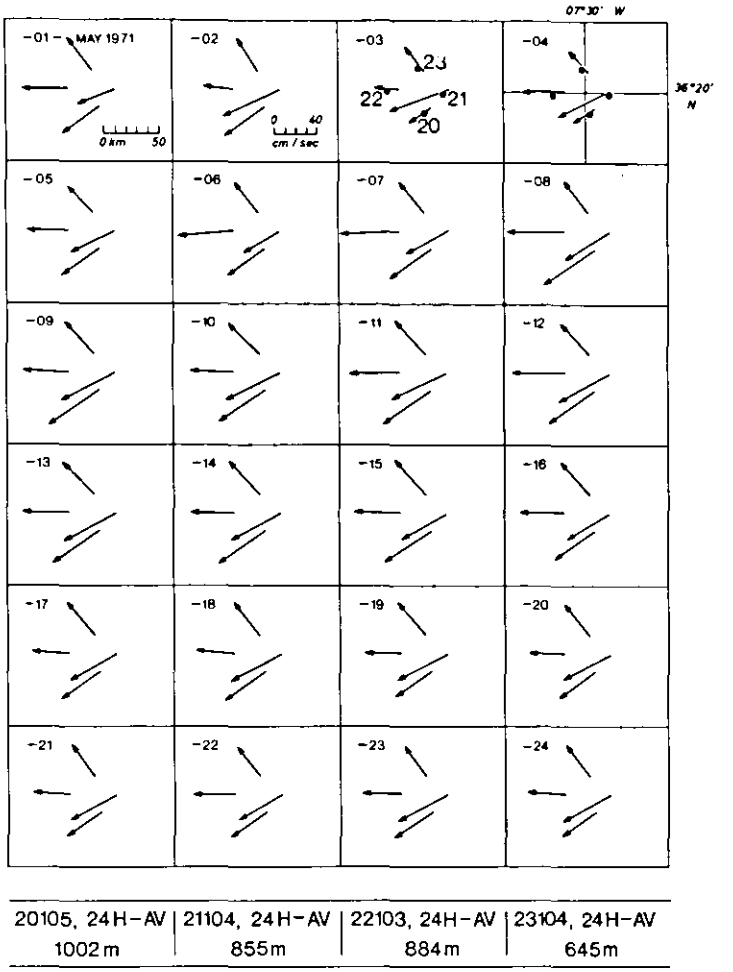

Fig. 5. Daily averaged current vectors in the core of the Mediterranean Outflow. Data from moorings 20—23 are shown for the time interval May 1 through May 24, 1971. The frames are centered arround 36° 20′ N and 07° 30′ W. For details compare with Table 1.

Abb. 5. Täglich gemittelte Stromvektoren in der Kernschicht des Mittelmeerausstromes. Daten der Verankerungen 20—23 sind dargestellt für den Zeitraum 1. Mai—24. Mai 1971. Der geographische Mittelpunkt der Einzelbilder liegt bei 36° 20′ N und 07° 30′ W. Weitere Erklärungen sind Tabelle 1 zu entnehmen.

of the shelf slope of Cape Santa Maria. Perpendicular to this outrunning channel lies Section B (Fig. 3). At station 47 the bottom rise indicates the western end of the depositional ridge which limits the shelf branch of Mediterranean water (Giesel & Seibold 1968).

The outflow mainly is concentrated on two regions, one on the southern and one on the northern side of the section. The southern core between stations 49 and 51 belongs to the intermediate branch discussed later while the northern part describes the hydrography of the shelf branch (between stations 44 and 47). The division of Section B also is evident from the weak geostrophic currents which become <2 cm sec^{-1} below 300 m between CTD stations 47 and 48. The different travel history of both branches was demonstrated by Kroebel (1973) by means of differences in light attenuation factors which were measured simultaneously with the T/S profiles.

The shelf branch shows a dual structure that splits it in an upper and in a lower part. The calculation of the effective cross section yields $0.18 \cdot 10^6$ m^2 for the upper and $1.65 \cdot 10^6$ m^2 for the lower core. In order to calculate the volumetric transport for the upper vein the mean geostropic velocity (13 cm sec^{-1}) had to be used while the integrated speed for the lower core was obtained from current meters 25 104 and 25 105 (23 cm sec^{-1}). The numbers yield the flux of $T_{25} = 0.40 \cdot 10^6$ m^3 sec^{-1}.

The mean current records as given in Table 1 show a direction parallel to the shelf in all cases reflecting the constraint by the southward projection of the shelf near Cape Santa Maria as mentioned by Kenyon & Belderson. The maximum value in the mean vertical current profile appears between 450 and 550 m depth although Section B shows no evidence of high currents in this depth range. An explanation for this disagreement might be found in the method of comparing a quasi-synoptic section with a monthly mean current profile. At least the temperature record of 25 101 shows the highest variance of all records which highlights the problem. The maximum observed speed appeared in 25 102 with 69 cm sec^{-1}.

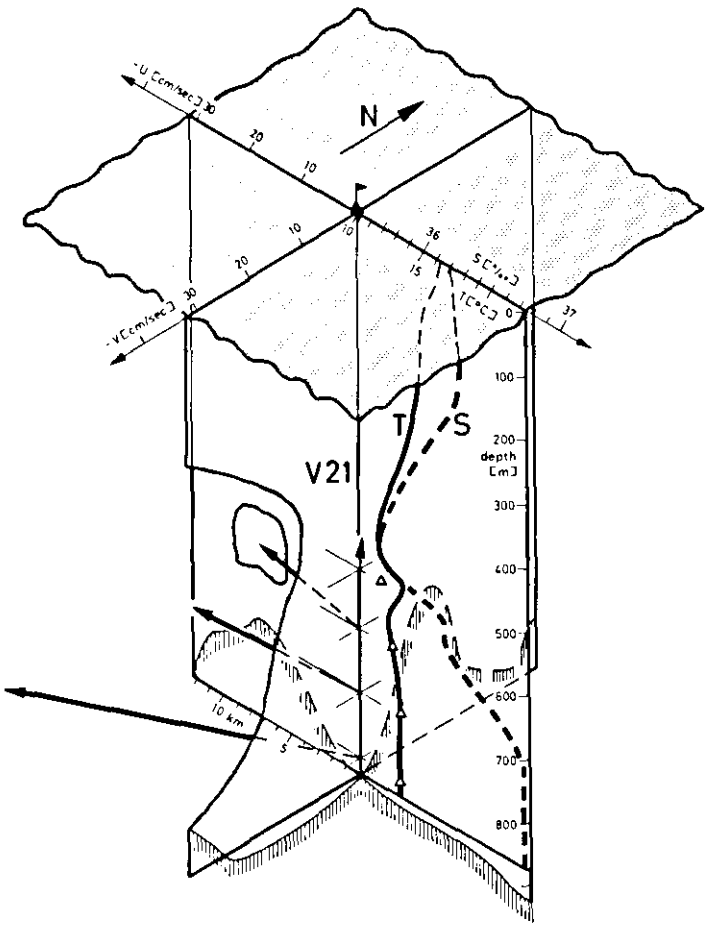

Fig. 6. Representation of hydrography (CTD station 6) and topography at mooring site 21. The core of the warm and highly saline Mediterranean outflow is strongly influenced by the local topography which causes a leftward veering of the current profile. The triangles (△)denote averaged temperatures according to Table 1.

Abb. 6. Darstellung von Hydrographie (Station 6) und Topographie bei Verankerung 21. Der Kern des warmen und salzreichen Mittelmeerausstromes steht unter dem Einfluß der lokalen Topographie. Diese bewirkt ein linksdrehendes Stromprofil. Die Dreiecke (△) kennzeichnen die gemittelten Temperaturen im Anschluß an Tabelle 1.

The intermediate branch (Section B)

The evidence of this outflow channel was already shown in cross section B together with the shelf branch (Fig. 3). Unfortunately no individual hydrographic section is available at the source of this branch. According to Figs. 1 and 4 it starts between two ridges both at depth of <600 m. The current records obtained from mooring 23 show a permanent northwesterly outflow in the depth range of Mediterranean Water (Fig. 5). The thickness of the outflow was observed to be approximately 150 m (CTD station 161). According to various topographic charts found in literature (HEEZEN & JOHNSON 1969, HEEZEN & HOLLISTER 1971, MADELAIN 1970, and KENYON & BELDERSON 1973) and obtained during the cruise (Fig. 4) one estimates 7.5 km, for the width of the channel. The current data in Table 1 give the mean outflow speed: 21 cm sec^{-1}. With these numbers the volumetric transport by the intermediate branch is $T_{23} = 0.23 \cdot 10^6$ m^3 sec^{-1}.

The effect of the intermediate branch on the sea bed has been shown in a photograph by MELIÉRES et al. (1970). During their observations a near bottom speed of 40 cm sec^{-1} was found which is consistent with record 23 104 (see Table 1).

The main branch (Section C)

This name was chosen because the area under consideration transports the largest part of the Mediterranean outflow. A representation of the characteristic hydrography and topography at the upper end of the main outflow branch is shown in Fig. 6. This picture combines the mean three dimensional current profile (mooring 21) with a single T and S-profile (CTD station 6). As the mean temperature values observed by the current meters indicate, the T-profile displayed here is rather typical for the location. Deviations between the continuous profile and the mean temperature profile appear only at the depth of the uppermost current meter (557 m) where the interface occasionally passed the sensor causing the high temperature variance of 21 101 (Table 1).

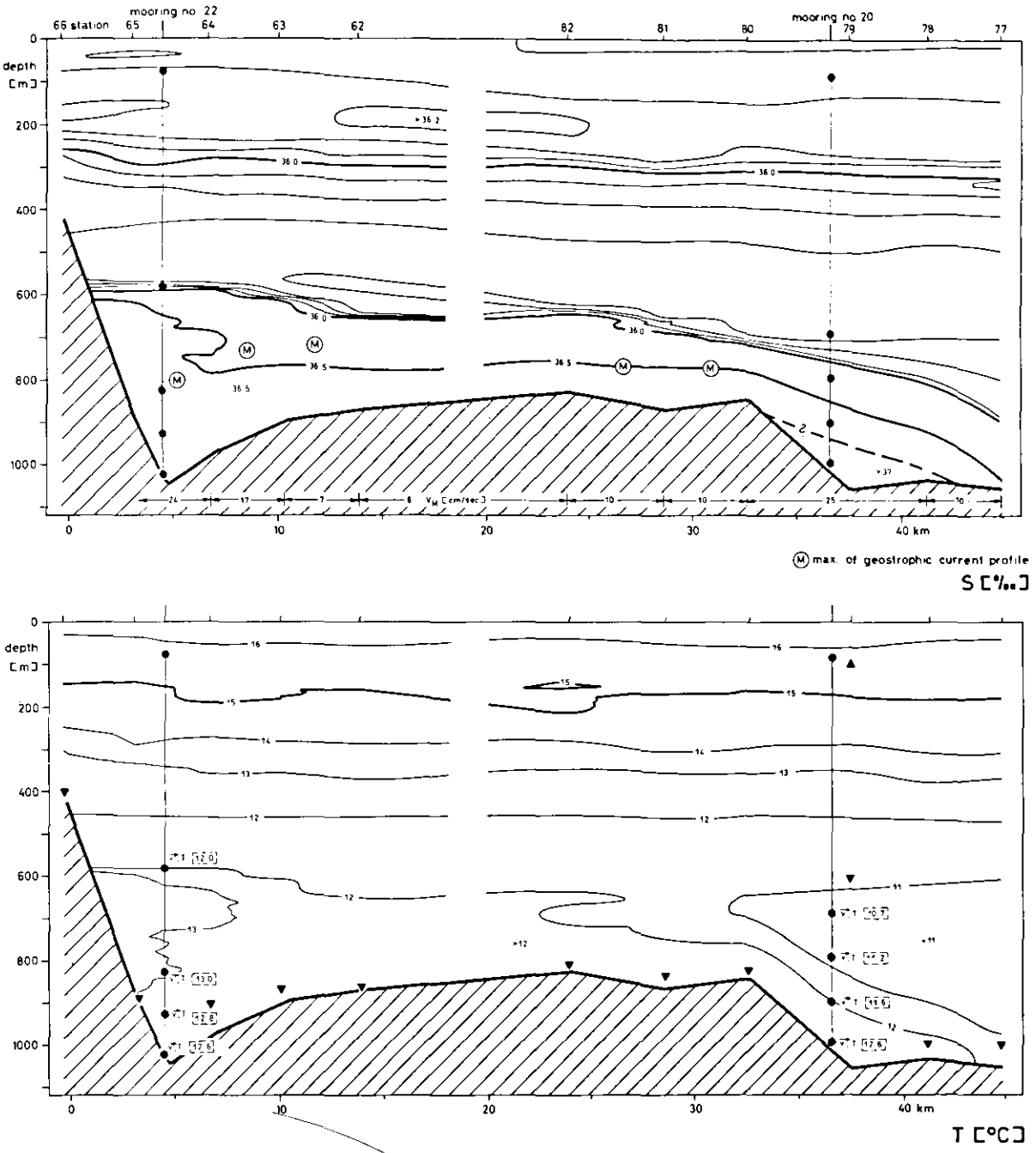

Fig. 7. Hydrographic section C through the main outflow branch of the Mediterranean outflow and positions of mooring sites 20 and 22. A time shift of 2.25 days is indicated by the gap between stations 62 and 82. Maxima of the calculated geostrophic currents are shown by (M). Vertically integrated speed values of the outflow are given under the salinity profile.

Abb. 7. Hydrographischer Schnitt C durch den Hauptausstromarm des Mittelmeerwassers zusammen mit den Verankerungspositionen 20 und 22. Eine Zeitverschiebung von 2,25 Tagen ist durch die Lücke zwischen den Stationen 62 und 82 angedeutet. Zur Kennzeichnung der Maxima der geostrophischen Ströme wurde das Symbol (M) verwendet. Vertikal integrierte Geschwindigkeitsbeträge des Ausstroms sind unterhalb des Salzgehaltschnittes eingetragen.

Finally from Figs. 4 and 6 the strong influence of the bottom topography on the outflow layer can be derived. The ridges found in the NW-square of Fig. 6 constrain the fast-flowing near-bottom core (Fig. 5) to be deflected more southward than the intermediate and upper layer of the outflow leading to the leftward veering of the current profile as observed.

Section C in Fig. 7 presents the situation at the lower branch of the main outflow together with

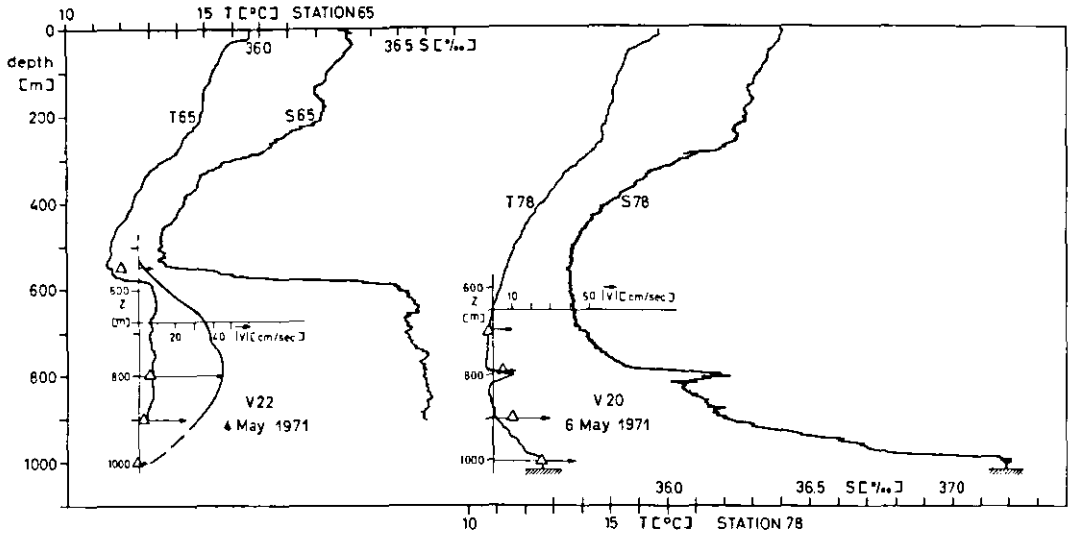

Fig. 8. CTD stations 65 and 78 together with the geostrophic current profile between station 64 and 65. The shown averaged speed and temperature values (△) (moorings 22 and 20) were obtained 12 hours prior to the adjacent hydrographic stations. The graph illustrates how the outflow core has already left the bottom at station 65, while it still touches the bottom at station 78 (compare with Fig. 7).

Abb. 8. Hydrosondenstationen 65 und 78 zusammen mit dem geostrophischen Stromprofil zwischen den Stationen 64 und 65. Die dargestellten Geschwindigkeits- und Temperaturwerte (△) aus den Verankerungen 22 und 20 wurden über 12 Stunden gemittelt. Sie stammen aus dem Zeitintervall vor den Messungen auf den benachbarten hydrographischen Stationen. Die Darstellung zeigt, wie der Kern des Ausstromes den Boden bei Station 65 bereits verlassen hat, während er bei Station 78 noch auf dem Boden liegt (vergleiche Abb. 7).

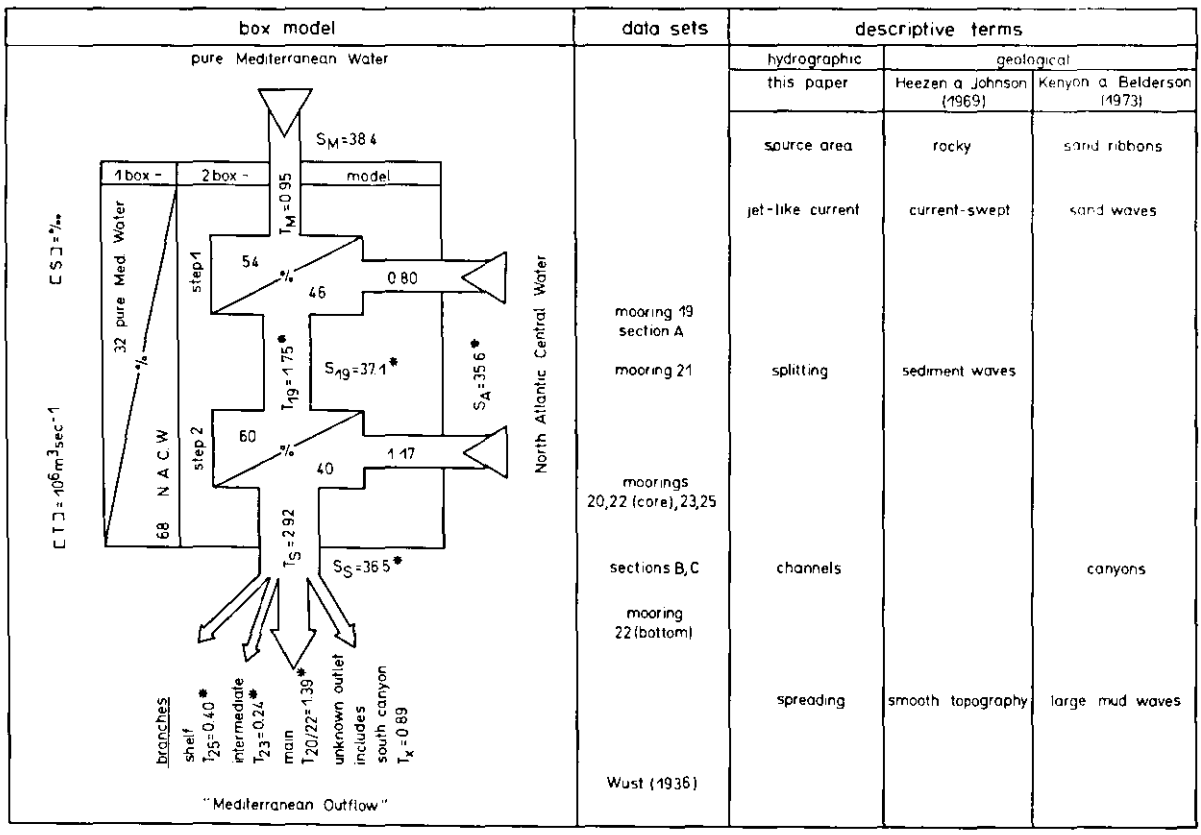

Fig. 9. The outflow cascade of the Mediterranean Water in the Gulf of Cádiz.
Abb. 9. Ausstromkaskade des Mittelmeerwassers im Golf von Cádiz.

moorings 20 and 22 and the relative maxima (M) of the geostrophic current profiles. The fact that the data from Section C were not obtained simultaneously is indicated graphically by the gap between station 62 and 82. The cross section obtained shows an uninterrupted band of outflow water which does not fit the picture of two separated outflow channels for that region as given by MADELAIN (1970).

The evidence for an uninterrupted flow between mooring arrays 22 and 20 is consistent with KENYON & BELDERSON's Fig. 19 that shows at 36° 22′ N, 07° 30′ W an outflow filament in between the channels displayed by MADELAIN (1970). Regarding the field of motion a significant difference between mooring sites 22 and 20 was observed.

While mooring 20 together with CTD station 78 (see Fig. 8) showed the same characteristics as mooring 19, i.e. maximum speed near the bottom, the outflow core has lost contact with the bottom in the region of mooring 22. At mooring 20 the highest average speed of 50 cm sec^{-1} was found at 1002 m near the bottom while the measured profile at 22 which fits the geostrophic calculation (Fig. 8) yields a maximum value of 39 cm sec^{-1} at approximately 800 m. As average intervalls the 12 hours prior to the affiliated CTD stations were chosen. In comparing the geostrophic current profile with the directly measured data a positive vertical correction of 80 m was necessary due to the more downstream position of mooring 22.

Similar to the previous calculation an estimate of the volumetric transport through Section C was carried out with the result of $T_{20\text{-}22} = 1.39 \cdot 10^6$ m^3 sec^{-1}. The calculation was done under the assumption that all the outflow of Mediterranean Water is perpendicular to the section. The obtained values of the vertically integrated geostrophic speed V_M and the locations of their maxima values are included in Fig. 7.

The region near mooring 22 has been investigated earlier by THORPE (1972) who showed pictures of a sediment cloud below the Mediterranean core. This observation under the jet-like outflow (see Figs. 5 and 8) is consistent with the low speed and low temperature values that were obtained from meter 22 105 (9 cm sec^{-1} and 12.6 °C). The variance of speed and temperature are remarkably low which favours the creation of the large mud waves as reported by KENYON & BELDERSON.

The south canyon branch

Although this outflow branch was not investigated during "Meteor" cruise 23, there are several indications for the permanent existence of a fourth filament which separates in a southward direction soon after passing the gateway at Section A.

At approximately 36° 00′ N, 07° 08′ W the bathymetric chart shows a sharp feature that is formed by a very steep canyon. Sonographs by KENYON & BELDERSON indicate an abnormally high slope and a canyon width of 1.5—2.0 km. Hydrographic stations close beside the channel show at the bottom nearly pure NACW (e.g. Discovery Station 3990, FUGLISTER, unpublished) similar to uninfluenced water of the Sargasso Sea in 500 m depth (e.g. Crawford station 231, FUGLISTER 1960). At the Discovery station (35° 58′ N, 07° 02′ W), a salinity of only 35.74‰ was observed 25 m above the bottom. This is a strong indication of the jet-like character of this outflow filament which leaves the surrounding water masses relatively unaffected.

KENYON & BELDERSON called this branch "the most problematic channel" because the geological features show the most intensive interaction between the sea floor and the undercurrent.

The geological observations confirm the hydrographic survey by MADELAIN (1970) who illustrated this branch as a narrow but separate outflow vein of highly saline Mediterranean Water.

No quantitative value for the transport through the canyon can be given. However, it is surely one reason for he poorly balanced budget of the total outflow discussed in the next paragraph.

The outflow cascade

In order to give a budget of the outflow of the Gulf of Cádiz the sum of the different outlets has to be compared with T_{19} at the gate way section. First of all, however, the mixing with NACW in the area must be taken into account: an estimate of the vertical averaged salinity profile weighted by the speed in Section A results in a salinity of $S_{19} = 37.1$‰. Similarly, one gets a salinity of $S_S = 36.5$‰ for the profiles in Sections B and C in the region of the outflow where its horizontal spreading starts. The salinity of water mixed with S_{19} to yield S_S is again $S_A = 35.6$‰. Consequently, the water that passes Section A ($1.75 \cdot 10^6$ m^3 sec^{-1}) as the Mediterranean undercurrent represents 60% of the product which is mixed with 40% NACW ($1.17 \cdot 10^6$ m^3 sec^{-1}) leading to a transport of $T_S = 2.92 \cdot 10^6$ m^3 sec^{-1} leaving the Gulf of Cádiz.

Fig. 9 illustrates the process between the Strait of Gibraltar and the outer edge of the Gulf of Cádiz in terms of a box model. The values that were observed during the investigation Meteor 23 are marked by (*). All other numbers are derived from these values. The figure shows how the mixing progresses in two steps (outflow cascade).

While the first step of the cascade has been described earlier (Section A), the second includes the portions in the channels investigated here, T_{25}, T_{23}, and $T_{20'22}$ as components of T_S. The measured parts sum up to $2.03 \cdot 10^6$ m^3 sec^{-1}. An undetermined outlet $T_X = 0.89 \cdot 10^6$ m^3 sec^{-1} had to be added to keep T_S in balance.

T_X cannot be supplied by the small south canyon branch alone. Besides the contribution from this filament of the outflow, several other reasons have certainly influenced the poorly balanced budget. Similar to the connection of the northern and the southern part of Section C there might exist a continuous layer of outflowing water between the southern end of Section C and the south canyon branch. Such a broad extension of Section C would be able to transport as much as the sum of $T_{20'22}$ and T_X. Other possible error sources are the insufficient knowledge of speed and salinity distribution, deviation from orthogonality between sections and the mean current directions, and synopsis problems.

However, a comparison between a recent study by WORTHINGTON (1975) and the results obtained here shows that $T_S = 2.9 \cdot 10^6$ m^3 sec^{-1} is in the right order of magnitude. WORTHINGTON postulates a transport of $3.0 \cdot 10^6$ m^3 sec^{-1} in the Mediterranean outflow to keep the Atlantic circulation balanced.

The continuation of the outflow cascade to a global scale was shown by WÜST (1936) by means of all available hydrographic data after the Meteor expedition 1925–27. He chose for the calculation of mixing between Mediterranean Water and Atlantic Water the following initial values: $S_{100} = 36.50‰$ and $S_0 = 34.68‰$. While S_{100} is equivalent to S_M as discussed here, it seems today to be more realistic to use for the other water mass the Sargasso Sea Water (S_A) rather than in the Weddel Sea Water (S_0). This correction at the lower end of the mixing line however, does not change the relative shape of the spreading of Mediterranean Water in the Atlantic published by WÜST (1936) in his Fig. XVI. Possible relative changes have been predicted by the author himself for the case of a variation of the upper end of his mixing line.

Acknowledgements

The experiment at sea and the data evaluation were supported by the Deutsche Forschungsgemeinschaft, Bonn-Bad Godesberg. I benefitted from discussions with G. SIEDLER and members of the Woods Hole Buoy Group. Illustrations were drafted by A. FRIES, and P. SMITH helped me in preparing the English translation.

References

DEACON, M. (1971): Scientists and the Sea 1650–1900. — Acad. Press, 445 pp.

FUGLISTER, F. C. (1960): Atlantic Ocean Atlas of temperature and salinity profiles and data from the International Geophysical Year of 1957–1958. — Woods Hole Oceanogr. Inst., Woods Hole, Mass.

GIESEL, W. & E. SEIBOLD (1968): Sedimentechogramme vom ibero-marokkanischen Kontinentalrand. — „Meteor" Forsch.-Ergebn., C, 1: 53–75.

HEEZEN, B. C. & G. L. JOHNSON (1969): Mediterranean Undercurrent and Microphysiography west of Gibraltar. — Bull. Inst. Oceanogr. Monaco **67** (1382): 95 pp.

HEEZEN, B. C. & C. D. HOLLISTER (1971): The face of the deep. — Oxford University Press, New York, 659 pp.

KENYON, N. H. & R. H. BELDERSON (1973): Bed forms of the Mediterranean undercurrent observed with side-scan sonar. — Sedimentary Geology **9**: 77–99.

KROEBEL, W. (1973): Die Kieler Multimeeressonde. — „Meteor" Forsch.-Ergebn., A, 12: 53–67.

LACOMBE, H., F. MADELAIN & J. C. GASCARD (1968): Rapport sur la campagne ‚Gibraltar I' du navire océanographique Jean Charcot, 7 avril–12 mai 1967. — Cah. Oc. **20** (2): 101–108.

MADELAIN, F. (1970): Influence de la topographie du fond sur l'écoulement Méditerranéen entre le Detroit de Gibraltar et le Cap Saint-Vincent. — Cah. Oc. **22** (1): 43–61.

MELIÈRES, F., W. D. NESTEROFF & Y. LANCELOT (1970): Étude photographique des fonds du golfe de Cadis. — Cah. Oc. **22** (1): 63–72.

SCHOTT, G. (1915): Die Gewässer des Mittelmeeres. — Ann. Hydrogr. Bln. **43** (1): 63–79.

— (1928): Die Wasserbewegungen im Gebiete der Gibraltarstraße. — J. Conseil **3** (2): 139–175.

SIEDLER, G. (1972): Nordost-Atlantik-Expedition 1971. „Meteor" Forsch.-Ergebn. A, 10: 79–95.

SMITH, P. C. (1973): The dynamics of bottom boundary currents in the ocean, Ph. D. thesis MIT/WHOI.

STOMMEL, H., H. BRYDEN & P. MANGELSDORF (1973): Does the Mediterranean outflow come from great depth? Pageoph **105** (4): 879–889.

THORPE, S. A. (1972): A sediment cloud below the Mediterranean outflow. — Nature, Lond. **239**: 326–327.

— (1973): An electromagnetic current meter to measure turbulent fluctuations near the ocean floor. — Deep-Sea Res. **30**: 933–938.

WORTHINGTON, L. V. (1975): On the North Atlantic Circulation. — The Johns Hopkins Oceanographic Studies (in press).

WÜST, G. (1936): Schichtung und Zirkulation des Atlantischen Ozeans. — Erg. dt. Atl. Exp., Meteor 1925–1927, **6** (1), de Gruyter, Bln. u. Leibz.

ZENK, W. (1970): On temperature and salinity structure of the Mediterranean Water in the Northeast Atlantic. — Deep-Sea Res. **17**: 627–632.

— (1971): Zur Schichtung des Mittelmeerwassers westlich von Gibraltar. — „Meteor" Forsch.-Ergebn. A, 9: 1–30.

— (1974): Some current and temperature observations in the Mediterranean outflow west of Gibraltar; a data report — „Meteor" Forsch.-Ergebn. A, 15: 20–48.

Received Juli 5, 1974